ACS OMEGA

Article

Cite This: ACS Omega 2018, 3, 1897−1903

Ultrafine Highly Magnetic Fluorescent γ-Fe_2O_3/NCD Nanocomposites for Neuronal Manipulations

Vijay Bhooshan Kumar,*,† Michal Marcus,‡ Ze'ev Porat,§,∥ Lior Shani,⊥ Yosef Yeshurun,⊥ Israel Felner,# Orit Shefi,‡ and Aharon Gedanken*,†

†Bar-Ilan Institute for Nanotechnology and Advanced Materials, Department of Chemistry, ‡Bar-Ilan Institute for Nanotechnology and Advanced Materials, Faculty of Engineering, and ⊥Bar-Ilan Institute for Nanotechnology and Advanced Materials, Department of Physics, Bar-Ilan University, Ramat Gan 5290002, Israel

§Institute of Applied Research, Ben-Gurion University of the Negev, Be'er Sheva 8410501, Israel

∥Division of Chemistry, Nuclear Research Center Negev, Be'er Sheva 8419001, Israel

#Racah Institute of Physics, The Hebrew University, Jerusalem 9190401, Israel

Supporting Information

ABSTRACT: In this work, we describe a low-cost, two-step synthesis of composites of nitrogen-doped carbon quantum dots (NCDs) with γ-Fe_2O_3 (NCDs/γ-Fe_2O_3), which is based on a hydrothermal cum co-precipitation method. The product is a fine powder of particles having an average diameter of 9 ± 3 nm. The physical and chemical properties of NCDs/γ-Fe_2O_3 were studied, as well as the superconducting quantum interference device and Mossbauer analysis of the magnetic properties of these nanocomposites. The interaction of NCDs/γ-Fe_2O_3 nanocomposites with neuron-like cells was examined, showing efficient uptake and low toxicity. Our research demonstrates the use of the nanocomposites for imaging and for controlling the cellular motility. The NCDs/γ-Fe_2O_3 nanocomposites are promising because of their biocompatibility, photostability, and potential selective affinity, paving the way for multifunctional biomedical applications.

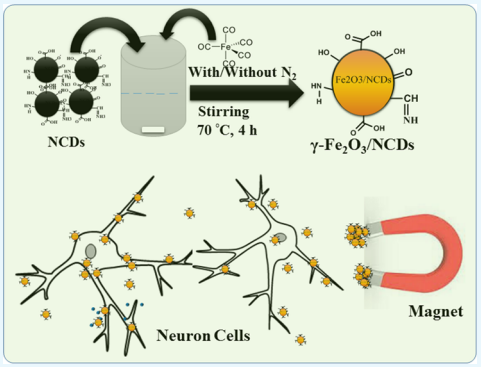

INTRODUCTION

Nanoscale materials are emerging as a new area of research that shows enormous potential for biological and clinical sciences. Among the advanced nanomaterials used in fundamental and applied research, carbon materials are some of the cheapest and most abundant in our surroundings.[1] Recently, fluorescent carbon nanoparticles, namely, carbon quantum dots (CDs), have attracted the attention of the scientific community because of their unique optical and electronic properties.[2] Moreover, the CDs have low toxicity, outstanding water solubility, and biocompatibility.[3] The fluorescence of CDs can be improved by nitrogen doping, and such nitrogen-doped CDs (N@CDs, or NCDs) have already been tested for various applications including fluorescent ratiometric, pH sensing,[4] in vivo bioimaging, drug delivery, and photocatalysis.[5−7] Hydrothermal synthesis is one of the commonly used methods for preparing CDs and doped CDs.[8,9]

Another attractive class of nanoparticles is magnetic nanoparticles, iron oxides (Fe_xO_y) are an example. Iron oxides are important transition-metal oxides. Because of their magnetic properties, they can be controlled by external magnetic fields. Currently, iron oxide nanomaterials are utilized in various biomedical applications, both in vitro and in vivo, including biomagnetic separation, magnetic resonance imaging (MRI) contrast,[10] hyperthermia, cell imaging,[11] and drug delivery.[12,13] Specifically, iron oxide nanoparticles were shown to be effective for neuronal repair and regeneration as they bestow promising capabilities for remote guidance of neuronal motility and growth.[14] Recent studies have demonstrated the use of iron oxide nanoparticles for directing the orientation of neurite growth during regeneration.[15,16] Iron oxide nanoparticles have also been used to guide progenitor neural cells through the blood stream toward injured sites using an external magnet.[17,18] Providing nanoparticles with fluorescence properties enables to trace the location of these nanoparticles in cells or tissues during cell imaging, disease analysis, and drug-targeting studies.[19] There are only a few reports in the literature on the synthesis of Fe_2O_3/CDs composites. Ma et al. have just simply synthesized the functional magnetic fluorescent Fe_3O_4/CDs composites by the thermal decomposition method.[20] Recently, Pramanik et al. reported the fluorescent magnetic CDs nanoparticles for efficient separation, differentiation, and eradication of superbugs.[21] It is well-known that doping CDs with nitrogen enhances their quantum yield. So far, CDs have been used mainly for fluorescence-based diagnostics. The magnetic CDs were prepared to expand the range of biomedical

Received: October 30, 2017
Accepted: January 29, 2018
Published: February 13, 2018

DOI: 10.1021/acsomega.7b01666
ACS Omega 2018, 3, 1897−1903

applications for which CDs can be used beyond bioimaging, for example, being used in MRI.

In this work, we report on a two-step synthesis of multifunctional γ-Fe_2O_3/NCD hybrid nanocomposites. The NCDs were synthesized from an aqueous solution of bovine serum albumin (BSA) by a hydrothermal reaction followed by the second step of co-precipitation with $Fe(CO)_5$. We propose a mechanism for the formation of these hybrid nanocomposites and investigate the long-lasting stability of their fluorescence and magnetization. These properties were found to be stable for more than four months. This remarkable stability is reflected in the fluorescence as well as in the absence of precipitation. We demonstrate the use of the nanocomposites for labeling neuron-like cells and for controlling their motility by applying an external magnetic field. These new NCDs/γ-Fe_2O_3 composites exhibit low toxicity and good biocompatibility and may therefore be beneficial as theranostic agents in various biomedical applications.

RESULTS AND DISCUSSION

The fine synthesized precipitates had a brownish red color and were analyzed by various physicochemical techniques and subsequently exploited for long-lasting stability examination as well as for an assessment of their biocompatibility. The γ-Fe_2O_3/NCDs hybrid nanocomposites were used as a probe for fluorescence imaging of neuron-like cells (PC12 and SHSY-5Y), and their potential for assisting neuronal differentiation was examined.

Physical and Chemical Characterization of γ-Fe_2O_3/NCDs. The γ-Fe_2O_3/NCDs nanocomposites were analyzed by various methods, including X-ray diffraction (XRD), UV, fluorescence, dynamic light scattering (DLS), zeta potential measurements, superconducting quantum interference device (SQUID), transmission electron microscopy (TEM), and energy-dispersive X-ray spectroscopy (EDS). XRD analysis indicated that the particles were highly crystalline with peaks matching the JCPDS powder diffraction file of γ-Fe_2O_3 (no. 65-3107). It also indicated the incorporation of γ-Fe_2O_3 in the NCDs. The presence of γ-Fe_2O_3 was identified in the products of the reactions with various ratios of reactants, as indicated by the similar XRD patterns (Figure 1). Therefore, herein, only the reaction with a 1:1 ratio ($Fe(CO)_5$ and NCDs) is discussed. XRD was also used to study the stability of the composite after different time points. It can be seen in Figure 1 that the XRD pattern remains almost identical even after 4 months in which the composite was kept at ambient conditions, indicating the air stability of the product. The XRD pattern of γ-Fe_2O_3 (Figure 1e) is similar to that of γ-Fe_2O_3/NCDs nanocomposites. The broad nature of all the diffraction peaks is due to the small size of the γ-Fe_2O_3/NCDs nanocomposites and NCDs (Figure 1f).

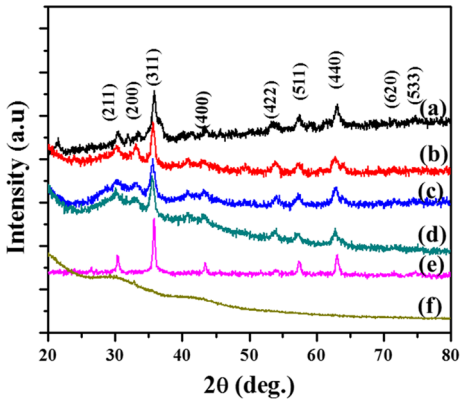

Figure 1. The XRD pattern of γ-Fe_2O_3/NCDs nanocomposites at ratios of (a) 1:2, (b) 1:1, (c) 2:1, (d) after 3 months (1:1 ratio), (e) pristine γ-Fe_2O_3 and (f) NCDs.

The magnetic properties of γ-Fe_2O_3/NCDs nanocomposites were characterized by SQUID and Mossbauer measurements at 300 K. Figure 2a depicts the measured magnetization curves demonstrating the superparamagnetic characteristics of the γ-Fe_2O_3/NCDs nanocomposites, with saturation magnetization values of $M_s \approx 35$ (2:1), 32 (1:1), and ~21 (1:1) emu/g of the products. On the basis of the XRD (Figure 1) and SQUID (Figure 2a) analyses, we identified the best sample as 1:1 ($Fe(CO)_5$/NCDs) with the highest saturation magnetization. In addition, we measured the magnetization of γ-Fe_2O_3/NCDs after 3 and 4 months and found that the value of M_s was hardly changed (from 32 to 31 emu/g, Figure 2). Hence, we conclude that γ-Fe_2O_3/NCDs are highly stable materials at room temperature and normal pressure. To determine the exact phase of the iron in the γ-Fe_2O_3/NCDs, we performed a Mossbauer analysis. The Mossbauer spectra of the γ-Fe_2O_3/NCDs are presented in Figure 2b, showing a sextet with an isomer shift [δ], line width, and effective hyperfine magnetic field [H_{eff}] values of 0.44 ± 0.01 mm·s^{-1}, 0.32 ± 0.04 mm·s^{-1}, and 487 ± 0.1 kOe, which is in accordance with γ-Fe_2O_3. The relative large line width indicates distribution of hyperfine parameters and may also correspond to large blocked particles.

The morphology of γ-Fe_2O_3/NCDs was observed by TEM (Figure 3). Spherical γ-Fe_2O_3/NCDs with sizes in the range of ~9 ± 3 nm were observed in the high-resolution TEM (HRTEM) image (Figure 3c), which is close to the typical size range of pristine CDs, indicating that the γ-Fe_2O_3 dopant has a rather small effect in terms of the size and the shape of the nanoparticles. The selected area electron diffraction (SAED, Figure 3d) reveals the phases of both NCDs (200)[22,23] and γ-Fe_2O_3 (311, 400).[24,25] The size distribution of γ-Fe_2O_3/NCD particles was assessed also by DLS measurements, which showed that the main population was within the size range of 12−20 nm with a peak corresponding to 14 nm, which is in a good agreement with the TEM observation (Figure S1, see the Supporting Information).

The fluorescence and absorption spectra of γ-Fe_2O_3/NCDs (Figure 4) confirm that the synthesized materials are fluorescent with high magnetization. Figure 4a shows the fluorescence spectra of the bare NCD particles, and Figure 4b shows the fluorescence spectra at different excitation wavelengths (330, 350, 370, 390, 410, 430, 450, and 470 nm). The fluorescence intensity of γ-Fe_2O_3/NCDs is reduced, and a blue shift of the emission with respect to NCDs is observed. An excitation spectrum was recorded also for γ-Fe_2O_3/NCDs, revealing a peak at 350 nm when the emission was collected at 430 nm, in support of the UV−vis analysis (Figure 4d).

Plausible Speculative Formation Mechanism of γ-Fe_2O_3/NCDs. A speculative hypothesis for the synthesis of γ-Fe_2O_3/NCDs from commercial iron pentacarbonyl is mixed with an aqueous suspension of NCDs in the presence of air; the $Fe(CO)_5$ decomposes at 70 °C in oxygen atmosphere to metallic iron nanoparticles, which act as initiators for the growth of Fe/NCDs. All clustered metallic iron atoms are oxidized to Fe_2O_3 to obtain γ-Fe_2O_3/NCDs as the final product. The γ-Fe_2O_3/NCDs nanocomposites are made more permeable during this process because of expansion upon

DOI: 10.1021/acsomega.7b01666
ACS Omega 2018, 3, 1897−1903

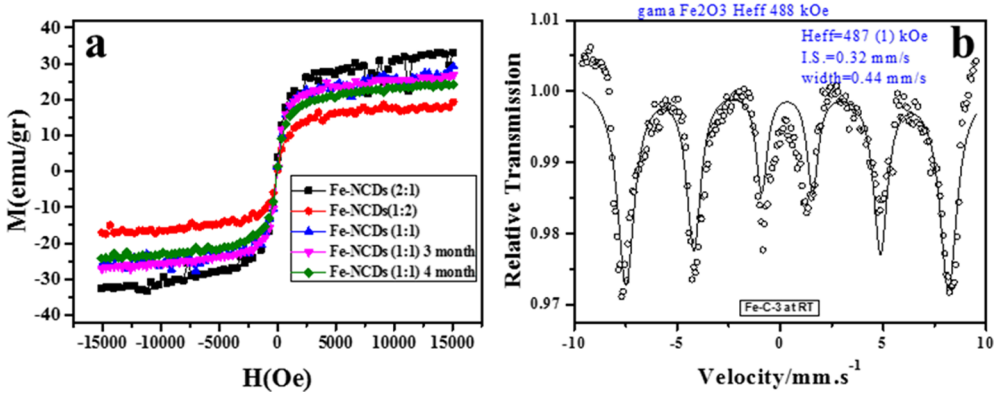

Figure 2. Magnetization analysis of γ-Fe_2O_3/NCDs. (a) SQUID measurements for different Fe_2O_3/NCD ratios (2:1, 1:2 and 1:1) and after 3 and 4 months (for the 1:1 ratio). (b) Mossbauer analysis for the 1:1 Fe_2O_3/NCD nanocomposite.

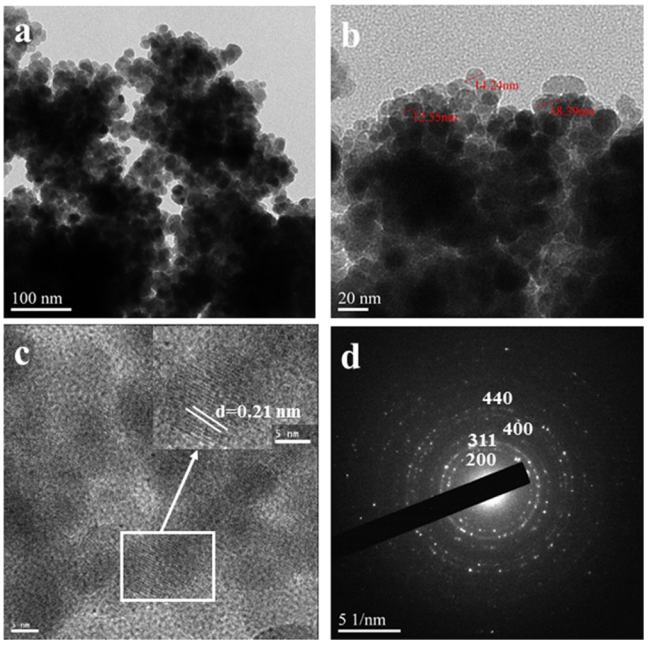

Figure 3. TEM image of the 1:1 γ-Fe_2O_3/NCD nanocomposite at (a) low magnification and (b) high magnification. (c) HRTEM images (inset: lattice fringes), and (d) SAED with marked lattice plane.

oxidation. Moreover, the NCD oxygen functional groups facilitate the nucleation and growth of the Fe_2O_3 nanoparticles.

Interaction of γ-Fe_2O_3/NCD Nanocomposites with the Living Cells. XTT cell viability assay was performed to examine the cytotoxicity of the γ-Fe_2O_3/NCDs. We tested the effect of γ-Fe_2O_3/NCDs on the viability of PC12 neural cells. The cells were incubated with γ-Fe_2O_3/NCDs at concentrations ranging from 0.05 to 0.5 mg/mL. Viability experiments were performed at time points 24 and 72 h after exposure to γ-Fe_2O_3/NCDs, and the results were normalized to the control cells without nanoparticles. PC12 cells that were treated with γ-Fe_2O_3/NCDs remained viable even after 72 h. No significant difference in cell viability was observed at all doses (Figure 5a), indicating that the γ-Fe_2O_3/NCDs are not cytotoxic to PC12 cells. The cells treated with γ-Fe_2O_3/NCDs also retained their ability to differentiate (Figure 5b); they demonstrated neurite outgrowth and formed a network, similar to control networks and to cells treated with other nanoparticles, as we have shown previously.[14,26] Different types of iron oxide nanoparticles demonstrate diverse cytotoxic effects. Some particles are found to be toxic even at low concentrations, whereas others exhibit biocompatible properties. The toxicity of iron oxide particles depends on many factors including particle stability, coating, and level of aggregation.[27−29] The remarkable biocompatibility of the γ-Fe_2O_3/NCDs enables us to use them in biological applications.

We then studied the uptake of γ-Fe_2O_3/NCDs by the cells and the effect of the concentration on the cellular uptake. PC12 cells were incubated for 24 h with γ-Fe_2O_3/NCDs at various concentrations (0.05−0.5 mg/mL), and the intracellular fluorescence intensity was measured by flow cytometry. Figure 6a shows the uptake of the γ-Fe_2O_3/NCDs nanocomposites by the cells; as can be seen in Figure 6b, the fluorescence increases proportionally with increasing γ-Fe_2O_3/NCDs concentrations.

Because of their fluorescent properties, γ-Fe_2O_3/NCDs can be detected within cells by fluorescent confocal microscopy. To verify particles' internalization into cells, we performed *z*-stack imaging and examined images at an intracellular focal plane. We compared between cells incubated with different particles: NCDs, Fe_2O_3 particles, or γ-Fe_2O_3/NCDs composites. Figure 7 presents confocal microscopy images of the cells at a single focal plane demonstrating the internalization of the particles into the cells. A fluorescent signal is observed in cells incubated with NCDs (Figure 7b) and in cells incubated with γ-Fe_2O_3/NCDs (Figure 7d). On the contrary, no fluorescence is detected in cells incubated with Fe_2O_3 particles (Figure 7c), similar to control cells without any particles (Figure 7a). Cell viability assay examined the cytotoxicity of NCDs and Fe_2O_3 particles at concentrations ranging from 0.05 to 0.25 mg/mL. No significant difference in cell viability was observed at all doses after 24 h (Figure S3, Supporting Information). The incorporation of γ-Fe_2O_3/NCDs within cells enables magnetic cell manipulations. As a proof of the concept, an external permanent magnet was placed at one side of the culture dish. Time-lapse observations demonstrated the movement of the γ-Fe_2O_3/NCD-treated cells toward the magnet (Figure S4, Supporting Information).

CONCLUSIONS

In summary, we have successfully synthesized γ-Fe_2O_3/NCD magnetic nanoparticles with high fluorescence and very good biocompatibility. The detailed formation is reported, along with a physical and chemical analysis. These fluorescent magnetic nanoparticles were also shown to be efficient for various neuronal manipulations, including cell labeling and controlled cell motility by means of magnetic force. The present approach

DOI: 10.1021/acsomega.7b01666
ACS Omega 2018, 3, 1897−1903

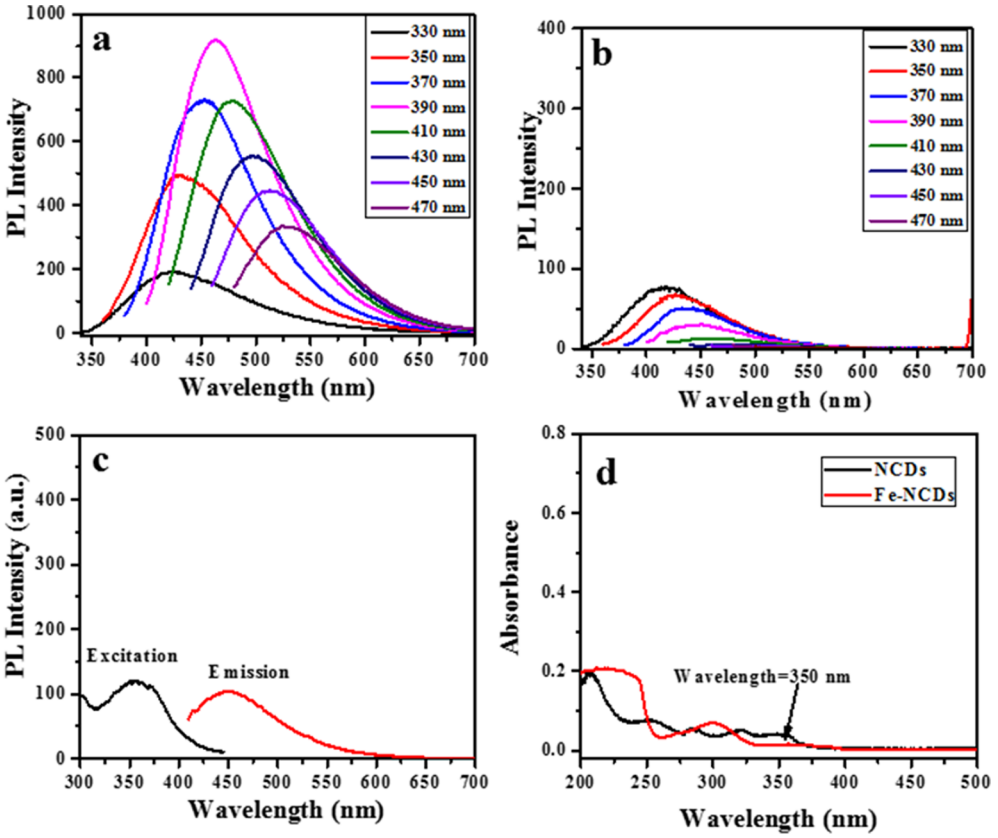

Figure 4. (a) Fluorescence spectra of (a) NCDs and (b) γ-Fe_2O_3/NCDs (1:1) as a function of the excitation wavelength. (c) Excitation and emission spectra of γ-Fe_2O_3/NCDs (1:1) and (d) absorption spectrum of NCDs and γ-Fe_2O_3/NCDs (1:1).

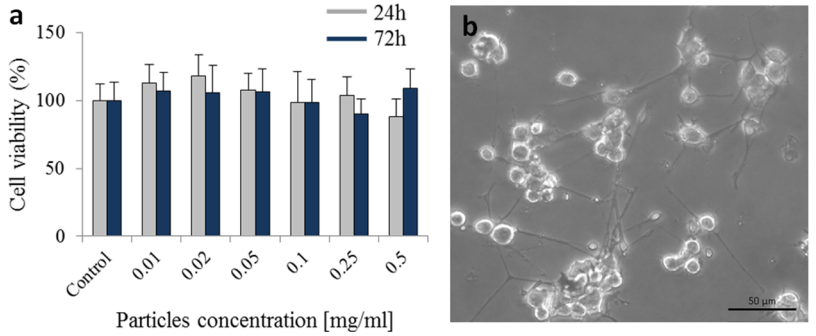

Figure 5. (a) XTT viability assay of PC12 cells incubated with increasing concentrations of γ-Fe_2O_3/NCDs after 24 and 72 h of incubation (n = 3). Results are normalized to control without NCDs. (b) Light microscopy image of PC12 cells treated with γ-Fe_2O_3/NCDs after four days of differentiation.

offers new insight into the production of cheap, highly sensitive, and selective materials for various biomedical applications.

EXPERIMENTAL METHODS

Chemicals. BSA, iron pentacarbonyl ($Fe(CO)_5$), and quinine sulphate were purchased from Sigma-Aldrich Ltd., Israel. Double-distilled water was used throughout the experiments. RPMI medium, horse serum (HS), fetal bovine serum (FBS), L-glutamine, penicillin−streptomycin, and amphotericin were purchased from Biological Industries, Israel. Murine β-NGF was purchased from Peprotech Ltd., Israel.

Synthesis of NCDs and γ-Fe_2O_3/NCD Nanocomposites. The preparation of the NCDs was done by a modified hydrothermal method starting from an aqueous solution of BSA (0.5 w/v %).[8] The procedure included dissolution of 0.30 g of BSA (66.5 kD) in 60 mL of ultrapure water and stirring for 10 min at room temperature. The resulting 0.5 w/v % solution was transferred into a 100 mL Teflon-lined autoclave and heated at 195 °C for 6 h in a hot-air oven. After completion, the reaction was quenched by cooling the autoclave in water. The large carbide slag was separated from the product solution by centrifugation at 12 000 rpm for 10 min. A pale-yellow homogeneous transparent suspension of NCDs was obtained. The concentration of the NCDs was determined by UV−vis spectroscopy and was found to be 5 mg/mL. This suspension (10−40 mL) was mixed with 10 mL of solution of iron pentacarbonyl at 70 °C with stirring for 4 h under air or N_2 atmosphere, and it was found that more precipitates were obtained under air. As stirring was stopped, red-brown particles started to precipitate. Three different volumes of the NCD

DOI: 10.1021/acsomega.7b01666
ACS Omega 2018, 3, 1897−1903

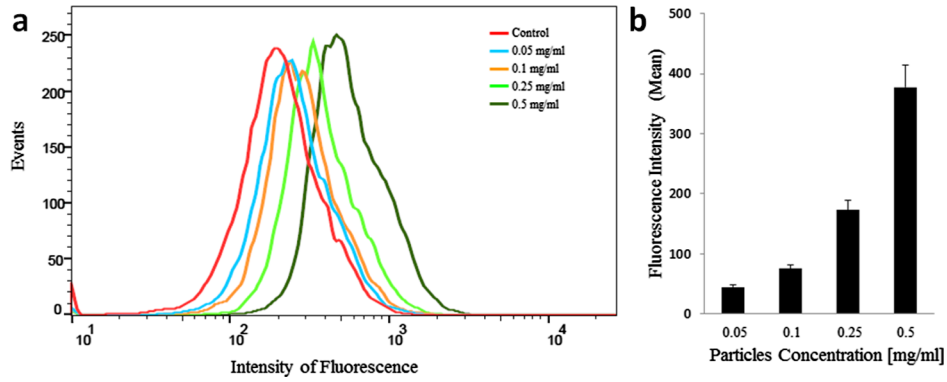

Figure 6. Cellular uptake of γ-Fe_2O_3/NCDs by PC12 cells; (a) fluorescence intensity measurements from cell cytometry of PC12 cells incubated with γ-Fe_2O_3/NCDs, ranging from 0.05 to 0.5 mg/mL, for 24 h. (b) Average of fluorescence intensity normalized to control without NCDs upon incubation of the cells with γ-Fe_2O_3/NCDs.

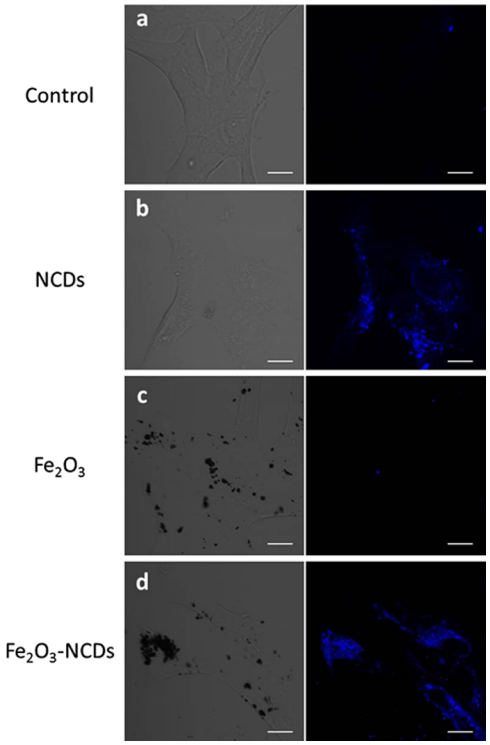

Figure 7. Confocal microscope image of SH-SY5Y cells treated with (a) no particles; (b) NCDs; (c) γ-Fe_2O_3 particles; (d) γ-Fe_2O_3/NCDs. Left: Bright field imaging. Right: Fluorescent imaging (excitation at 405 nm, emission at 450 ± 50 nm). Scale bar = 10 μm.

suspensions were used to examine the effect of the reactant weight ratios (2:1, 1:1, and 1:2) on the product. The composite particles were separated by evaporation of the water at 70 °C. A detailed schematic representation of the reaction that takes place is shown in Scheme 1.

Cell Culture. Rat pheochromocytoma PC12 cells (ATCC) were cultivated in suspension in RPMI medium supplemented with 10% HS, 5% FBS, 1% L-glutamine, 1% penicillin–streptomycin, and 0.2% amphotericin. The neuron cells were cultured in a 5% CO_2-humidified incubator at 37 °C. To induce differentiation, cells were seeded on collagen type I-coated plates and incubated for 24 h in serum-reduced medium (1% HS). A day after plating, murine β-NGF (50 ng/mL) was added to the cultures. The medium with added β-NGF was replaced every 2–3 days.

Scheme 1. Plausible Mechanism for the Formation of the γ-Fe_2O_3/NCDs Nanocomposites

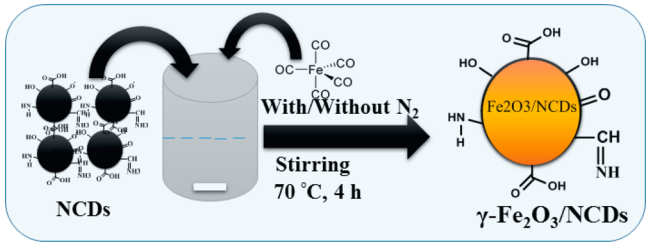

Flow Cytometry Analyses of Cellular Uptake. PC12 cells were incubated with γ-Fe_2O_3/NCDs at concentrations of 0.05, 0.10, 0.25, and 0.50 mg/mL. After 24 h, the cells were washed twice with fresh medium and collected in the dark. The fluorescence intensity was measured by flow cytometry (FACSAria III, BD Bioscience, USA) with laser excitation at 405 nm and emission-filtered at 450 nm, with 40 nm band width.

Cell Viability Assay. The XTT assay was used for a quantitative assessment of the toxicity of the γ-Fe_2O_3/NCDs. The XTT assay is based on the ability of metabolic active cells to reduce the tetrazolium salt XTT to orange colored compounds of formazan. The intensity of the dye is proportional to the number of metabolic active cells. PC12 cells were seeded on 96-well plates with γ-Fe_2O_3/NCDs at different concentrations and cultured for 24 and 72 h. XTT reaction solution (Biological Industries, Israel) was then added to the wells and incubated for 5 h at 37 °C. Absorbance was measured at 450 nm (630 nm background) using a spectrophotometer (BioTek Synergy 4, Vermont, USA).

Instruments and Analytical Techniques. UV–vis spectra of γ-Fe_2O_3/NCDs were measured using a Cary 100 spectrophotometer (Varian) operated by Labsphere software. The fluorescence of the γ-Fe_2O_3/NCDs suspension in water was measured by a fluorescence spectrophotometer (Varian Cary Eclipse). The functional group of γ-Fe_2O_3/NCDs was analyzed by a Fourier transform infrared spectrophotometer (Bruker TENSOR 27, platinum ATR diamond F) in the range of 4000–400 cm^{-1}. Elemental analysis was performed by EDS using a transmission electron microscope. HRTEM analysis was carried out on a JEOL 2100 microscope, which was operated at an accelerating voltage of 200 kV. The samples for TEM were prepared by dropping an aqueous solution of γ-Fe_2O_3/NCDs in isopropanol on a gold-coated copper TEM grid and then dried

DOI: 10.1021/acsomega.7b01666
ACS Omega 2018, 3, 1897–1903

under vacuum at room temperature overnight. The C, H, N, S, and O analyses were performed by CHNSO/O chromatogram spectroscopy. Zeta potential measurements of the particles, as well as their size distribution studies were performed on a ZetaSizer Nano-ZS (Malvern Instruments Ltd., Worcestershire, UK). The DLS was measured on the same instrument in an aqueous solution. X-ray powder diffractograms were obtained using a Bruker D8 ADVANCE diffractometer. Bragg−Bretano geometry was adopted using Cu Kα radiation (λ = 1.541 Å) and a setting of 40 kV and 40 mA. The phases were identified using the JCPDS database. The magnetization measurements were conducted by a Quantum Design MPMS5 SQUID magnetometer. The γ-Fe_2O_3 phase analysis was done using a Mossbauer spectrometer.

■ ASSOCIATED CONTENT

Supporting Information

The Supporting Information is available free of charge on the ACS Publications website at DOI: 10.1021/acsomega.7b01666.

γ-Fe_2O_3/NCD magnetic nanoparticle interactions with neuron cells (AVI)

DLS plot of NCDs and γ-Fe_2O_3/NCD magnetic nanoparticles, TEM image of NCDs, and cell viability assay of NCDs and Fe_2O_3 particles at concentrations ranging from 0.05 to 0.25 mg/mL (PDF)

■ AUTHOR INFORMATION

Corresponding Authors

*E-mail: vijaybhushan86@gmail.com (V.B.K.).

*E-mail: gedanken@biu.ac.il, aharon.gedanken@biu.ac.il (A.G.).

ORCID

Vijay Bhooshan Kumar: 0000-0001-7899-1463

Ze'ev Porat: 0000-0002-9862-449X

Orit Shefi: 0000-0001-6680-7390

Aharon Gedanken: 0000-0002-1243-2957

Notes

The authors declare no competing financial interest.

■ ACKNOWLEDGMENTS

The authors are grateful to Ortal Lidor-Shalev for help with the TEM measurements and to Dr. Ilana Perelshtein for the HRTEM measurements carried out at the Department of Chemistry of Bar-Ilan University, Israel.

■ ABBREVIATIONS

BSA, bovine serum albumin; DDW, double distilled water; EDS, energy dispersive X-ray spectroscopy; FBS, fetal bovine serum; FWHM, full-width at half-maximum; HR-TEM, high-resolution transmission-electron microscopy; NTP, room temperature and normal pressure; NCDs, nitrogen-doped carbon-dots; PBS, phosphate buffered saline; TP, two-photon; XRD, X-ray diffraction

■ REFERENCES

(1) Jariwala, D.; Sangwan, V. K.; Lauhon, L. J.; Marks, T. J.; Hersam, M. C. Carbon Nanomaterials for Electronics, Optoelectronics, Photovoltaics, and Sensing. *Chem. Soc. Rev.* **2013**, *42*, 2824−2860.

(2) Wang, R.; Lu, K.-Q.; Tang, Z.-R.; Xu, Y.-J. Recent Progress in Carbon Quantum Dots: Synthesis, Properties and Applications in Photocatalysis. *J. Mater. Chem. A* **2017**, *5*, 3717−3734.

(3) Hong, G.; Diao, S.; Antaris, A. L.; Dai, H. Carbon Nanomaterials for Biological Imaging and Nanomedicinal Therapy. *Chem. Rev.* **2015**, *115*, 10816−10906.

(4) Shi, W.; Li, X.; Ma, H. A Tunable Ratiometric Ph Sensor Based on Carbon Nanodots for the Quantitative Measurement of the Intracellular pH of Whole Cells. *Angew. Chem., Int. Ed.* **2012**, *51*, 6432−6435.

(5) Ye, Z.; Tang, R.; Wu, H.; Wang, B.; Tan, M.; Yuan, J. Preparation of Europium Complex-Conjugated Carbon Dots for Ratiometric Fluorescence Detection of Copper(II) Ions. *New J. Chem.* **2014**, *38*, 5721−5726.

(6) Niu, J.; Gao, H. Synthesis and Drug Detection Performance of Nitrogen-Doped Carbon Dots. *J. Lumin.* **2014**, *149*, 159−162.

(7) Amjadi, M.; Manzoori, J. L. Strong Enhancement of the Chemiluminescence of the Cerium(IV)-Thiosulfate Reaction by Carbon Dots, and Its Application to the Sensitive Determination of Dopamine. *Microchim. Acta* **2014**, *181*, 671−677.

(8) Kumar, V. B.; Sheinberger, J.; Porat, Z.; Shav-Tal, Y.; Gedanken, A. A Hydrothermal Reaction of an Aqueous Solution of BSA Yields Highly Fluorescent N Doped C-Dots Used for Imaging of Live Mammalian Cells. *J. Mater. Chem. B* **2016**, *4*, 2913−2920.

(9) Huang, L.; Yang, S.; Chen, L.; Chen, S. Hydrothermal Synthesis of Fluorescent Carbon Dots towards Ion Response and Silk Screen Patterns. *Chem. Lett.* **2015**, *44*, 1251−1253.

(10) Shen, Z.; Wu, A.; Chen, X. Iron Oxide Nanoparticle Based Contrast Agents for Magnetic Resonance Imaging. *Mol. Pharm.* **2017**, *14*, 1352−1364.

(11) Wolfbeis, O. S. An Overview of Nanoparticles Commonly Used in Fluorescent Bioimaging. *Chem. Soc. Rev.* **2015**, *44*, 4743−4768.

(12) Rodzinski, A.; Guduru, R.; Liang, P.; Hadjikhani, A.; Stewart, T.; Stimphil, E.; Runowicz, C.; Cote, R.; Altman, N.; Datar, R.; et al. Targeted and Controlled Anticancer Drug Delivery and Release with Magnetoelectric Nanoparticles. *Sci. Rep.* **2016**, *6*, 20867.

(13) Sutradhar, K. B.; Amin, M. L. Nanotechnology in Cancer Drug Delivery and Selective Targeting. *ISRN Nanotechnol.* **2014**, *2014*, 939378.

(14) Marcus, M.; Karni, M.; Baranes, K.; Levy, I.; Alon, N.; Margel, S.; Shefi, O. Iron Oxide Nanoparticles for Neuronal Cell Applications: Uptake Study and Magnetic Manipulations. *J. Nanobiotechnol.* **2016**, *14*, 37.

(15) Polak, P.; Shefi, O. Nanometric Agents in the Service of Neuroscience: Manipulation of Neuronal Growth and Activity Using Nanoparticles. *Nanomed. Nanotechnol. Biol. Med.* **2015**, *11*, 1467−1479.

(16) Riggio, C.; Calatayud, M. P.; Giannaccini, M.; Sanz, B.; Torres, T. E.; Fernández-Pacheco, R.; Ripoli, A.; Ibarra, M. R.; Dente, L.; Cuschieri, A.; et al. The Orientation of the Neuronal Growth Process Can Be Directed via Magnetic Nanoparticles under an Applied Magnetic Field. *Nanomed. Nanotechnol. Biol. Med.* **2014**, *10*, 1549−1558.

(17) Tewarie, R. S. N.; Hurtado, A.; Bartels, R. H.; Grotenhuis, A.; Oudega, M. Stem Cell-Based Therapies for Spinal Cord Injury. *J. Spinal Cord Med.* **2009**, *32*, 105−114.

(18) Clarke, J. L.; Daniell, H. Plastid biotechnology for crop production: present status and future perspectives. *Plant Mol. Biol.* **2011**, *76*, 211−220.

(19) NDong, C.; Tate, J. A.; Kett, W. C.; Batra, J.; Demidenko, E.; Lewis, L. D.; Hoopes, P. J.; Gerngross, T. U.; Griswold, K. E. Tumor Cell Targeting by Iron Oxide Nanoparticles Is Dominated by Different Factors in Vitro versus in Vivo. *PLoS One* **2015**, *10*, No. e0115636.

(20) Ma, Y.-j.; Liu, C.-y.; Zhou, X.-h.; Liu, Y. Preparation and Characterisation of Multifunctional Magnetic-Fluorescent Fe3O4/carbon Dots/silica Composites. *Micro Nano Lett.* **2013**, *8*, 302−304.

(21) Pramanik, A.; Jones, S.; Pedraza, F.; Vangara, A.; Sweet, C.; Williams, M. S.; Ruppa-Kasani, V.; Risher, S. E.; Sardar, D.; Ray, P. C. Fluorescent, Magnetic Multifunctional Carbon Dots for Selective Separation, Identification, and Eradication of Drug-Resistant Superbugs. *ACS Omega* **2017**, *2*, 554−562.

DOI: 10.1021/acsomega.7b01666
ACS Omega 2018, 3, 1897−1903

(22) Kumar, V. B.; Sahu, A. K.; Mohsin, A. S. M.; Li, X.; Gedanken, A. Refractive-Index Tuning of Highly Fluorescent Carbon Dots. *ACS Appl. Mater. Interfaces* **2017**, *9*, 28930−28938.
(23) Linehan, K.; Doyle, H. Size Controlled Synthesis of Carbon Quantum Dots Using Hydride Reducing Agents. *J. Mater. Chem. C* **2014**, *2*, 6025−6031.
(24) Kazeminezhad, I.; Mosivand, S. Phase Transition of Electro-oxidized Fe3O4 to γ And α-Fe2O3 Nanoparticles Using Sintering Treatment. *Acta Phys. Pol., A* **2014**, *125*, 1210−1214.
(25) Wu, W.; Xiao, X. H.; Zhang, S. F.; Peng, T. C.; Zhou, J.; Ren, F.; Jiang, C. Z. Synthesis and Magnetic Properties of Maghemite (γ-Fe2O3) Short-Nanotubes. *Nanoscale Res. Lett.* **2010**, *5*, 1474−1479.
(26) Marcus, M.; Skaat, H.; Alon, N.; Margel, S.; Shefi, O. NGF-Conjugated Iron Oxide Nanoparticles Promote Differentiation and Outgrowth of PC12 Cells. *Nanoscale* **2015**, *7*, 1058−1066.
(27) Pisanic, T. R.; Blackwell, J. D.; Shubayev, V. I.; Fiñones, R. R.; Jin, S. Nanotoxicity of Iron Oxide Nanoparticle Internalization in Growing Neurons. *Biomaterials* **2007**, *28*, 2572−2581.
(28) Mahmoudi, M.; Hofmann, H.; Rothen-Rutishauser, B.; Petri-Fink, A. Assessing the in Vitro and in Vivo Toxicity of Superparamagnetic Iron Oxide Nanoparticles. *Chem. Rev.* **2012**, *112*, 2323−2338.
(29) Connell, J. J.; Patrick, P. S.; Yu, Y.; Lythgoe, M. F.; Kalber, T. L. Advanced Cell Therapies: Targeting, Tracking and Actuation of Cells with Magnetic Particles. *Regener. Med.* **2015**, *10*, 757−772.

DOI: 10.1021/acsomega.7b01666
ACS Omega 2018, 3, 1897−1903